

One-bit Distributed Sensing and Coding for Field Estimation in Sensor Networks

Ye Wang, Prakash Ishwar, and Venkatesh Saligrama[†]

Abstract

This paper formulates and studies a general distributed field reconstruction problem using a dense network of noisy one-bit randomized scalar quantizers in the presence of additive observation noise of unknown distribution. A constructive quantization, coding, and field reconstruction scheme is developed and an upper-bound to the associated mean squared error (MSE) at any point and any snapshot is derived in terms of the local spatio-temporal smoothness properties of the underlying field. It is shown that when the noise, sensor placement pattern, and the sensor schedule satisfy certain weak technical requirements, it is possible to drive the MSE to zero with increasing sensor density at points of field continuity while ensuring that the per-sensor bitrate and sensing-related network overhead rate simultaneously go to zero. The proposed scheme achieves the order-optimal MSE versus sensor density scaling behavior for the class of spatially constant spatio-temporal fields.

I. INTRODUCTION AND OVERVIEW

We study the problem of reconstructing, at a data fusion center, a temporal sequence of spatial data fields, in a bounded geographical region of interest, from finite bit-rate messages generated by a dense noncooperative network of sensors. The data-gathering sensor network is made up of noisy low-resolution sensors at known locations that are statistically identical (exchangeable) with respect to the sensing operation. The exchangeability assumption reflects the property of an unsorted collection of inexpensive mass-produced sensors that behave in a statistically identical fashion. We view each data field as an unknown deterministic function over the geographical space of interest and make only the weak assumption that they have a known bounded maximum dynamic range. The sensor observations are corrupted by bounded, zero-mean, additive noise which is independent across sensors with arbitrary

[†] Y. Wang, P. Ishwar, and V. Saligrama are with the Department of Electrical and Computer Engineering, Boston University, Boston, MA 02215. Email: {yw, pi, srv}@bu.edu.

dependencies across field snapshots. This *noise has an arbitrary, unknown distribution* but a known maximum dynamic range. The sensors are equipped with binary analog-to-digital converters (ADCs) in the form of comparators with random thresholds which are uniformly distributed over the (known) sensor dynamic range. These thresholds are assumed to be independent across sensors with arbitrary dependencies across snapshots. These modeling assumptions partially account for certain real-world scenarios that include (i) the unavailability of good initial statistical models for data fields in yet to be well studied natural phenomena, (ii) unknown additive sensing/observation noise sources, (iii) additive model perturbation errors, (iv) substantial variation of preset comparator thresholds accompanying the mass-manufacture of low-precision sensors, (v) significant temperature fluctuations across snapshots affecting hardware characteristics, and (vi) the use of intentional dither signals for randomized scalar quantization.

Building upon prior results in [1], [2], and [3], we develop a simple coding and field reconstruction scheme based on one-bit scalar quantized samples of noisy observations. We characterize the associated scaling behavior of the MSE of field reconstruction with sensor density in terms of the local and global moduli of continuity of the underlying sequence of fields. This MSE characterization is for fixed, positive, and equal sensor coding rates (bits per sensor per snapshot). These achievable results reveal that for bounded, zero-mean, additive observation noise of unknown distribution, the MSE at every point of continuity of every field snapshot can be made to go to zero as sensor density increases while simultaneously sending the per-sensor bitrate and any sensing-related network rate overheads (e.g., sensor addresses) to zero. This is possible if the sensor placement and sampling schedule satisfy a certain uniformity property. This property ensures that the field estimate at any given spatial location is formed using the observations from increasingly many sensors that are located within a vanishingly smaller neighborhood of the location.

The MSE results of this work pertain to uniform pointwise convergence to zero, that is, for every spatial location of every field, unlike results pertaining to spatially and temporally averaged MSE which are more commonly encountered. The rate of decay of field reconstruction MSE at a given location is related to the local modulus of continuity of the field at the given location and time. Specializing these results to the case of spatially constant fields yields an achievable MSE decay rate of $O(1/N)$ where N is the sensor network size.¹ A Cramér–Rao lower-bound on the MSE for parameter estimation

¹Landau’s asymptotic notation: $f(N) = O(g(N)) \Leftrightarrow \limsup_{N \rightarrow \infty} |f(N)/g(N)| < \infty$; $f(N) = \Omega(g(N)) \Leftrightarrow g(N) = O(f(N))$; $f(N) = \Theta(g(N)) \Leftrightarrow f(N) = O(g(N))$ and $g(N) = O(f(N))$.

establishes that the $O(1/N)$ MSE scaling behavior is order-optimal in a minimax sense. Since in our problem formulation, the per-sensor bitrate is held fixed and equal across sensors, in a scaling sense, the MSE decreases inversely with the total network rate.

Previous estimation-theoretic studies of one-bit distributed field reconstruction have focused on reconstructing a single field snapshot and have either (i) assumed zero observation noise [1], [2], or (ii) assumed a spatially constant field (equivalent to scalar parameter estimation) with a one-bit communication as opposed to a one-bit sensing constraint [3]. The system proposed in this work integrates the desirable field sensing and reconstruction properties of these apparently different one-bit field estimation schemes and establishes the statistical and performance equivalence of these approaches. An important hardware implication of this paper is that noisy op-amps (noisy threshold comparators) are adequate for high-resolution distributed field reconstruction. This should be contrasted with the framework in [3] which implicitly requires sensors to have the ability to quantize their observations to an arbitrarily high bit resolution. A side contribution of this paper is the holistic treatment of the general distributed field-reconstruction problem in terms of (i) the field characteristics, (ii) sensor placement characteristics, (iii) sensor observation, quantization, and coding constraints with associated sensing hardware implications, (iv) transmission and sensing-related network overhead rates, and (v) reconstruction and performance criteria. We have attempted to explicitly indicate and keep track of what information is known, available, and used where and what is not.

The randomized scalar quantization model for the sensor comparators not only captures poor sensing capabilities but is also an enabling factor in the high-fidelity reconstruction of signals from quantized noisy observations. As shown in [4] in an information-theoretic setting, and alluded to in [2], the use of *identical* deterministic scalar-quantization (SQ) in all sensors will result in the MSE performance being fundamentally limited by the precision of SQ, *irrespective of increasing sensor density*, even in the absence of sensor observation noise.² However, our results further clarify that having “diversity” in the scalar quantizers, achieved, for example, through the means of an intentional random dither, noisy threshold, or other mechanisms, can achieve MSE performance that tends to zero as the density of sensors goes to infinity (Section III-A, Implications). Randomization enables high-precision signal reconstruction because zero-mean positive and negative fluctuations around a signal value can be reliably “averaged out” when there are enough independent noisy observations of the signal value. This observation is also corroborated by the findings reported in the following related studies [1]–[3], [5]–[8].

²The problem will persist even for identical block vector-quantization (VQ) with identical binning (hashing) operations.

The results of this work are also aligned with the information-theoretic, total network rate versus MSE scaling results for the CEO problem which was first introduced in [9] and thereafter studied extensively in the information theory literature (see [10], [11] and references therein). However, it should be noted that information-theoretic rate-distortion studies of this and related distributed field reconstruction (multiterminal source coding) problems typically consider stationary ergodic stochastic fields with complete knowledge of the field and observation-noise statistics, block-VQ and binning operations, and time and space-averaged (as opposed to worst-case) expected distortion criteria. In VQ, sensors are allowed to collect long blocks of real-valued field samples (of infinite resolution) from multiple field snapshots before a discrete, finite bit-rate VQ operation. The fields are often assumed to be spatially constant and independent and identically distributed (iid) across time (frequently Gaussian) and the observation noise is often assumed to be additive with a known distribution (frequently Gaussian) as in the CEO problem. It should also be noted that the MSE scaling results for the CEO problem in [10] are with respect to the total network rate where the number of agents (or sensors) has already been sent to infinity while maintaining the total network rate a finite value. Recent information-theoretic results for stationary fields under zero observation noise have been developed in [12], [13]. There is also a large body of work on centralized oversampled A-D conversion, e.g., see [14] and references therein. Our work does not explicitly address physical-layer network data transport issues. In particular, we do not consider joint source-channel coding strategies (however see remark before Section IV-A). For certain types of joint source-channel coding aspects of this and related problems, we refer the reader to the following references [15]–[20]. Networking issues such as sensor scheduling, quality of service, and energy efficiency may be found in [21] and references therein.

The rest of this paper is organized as follows. The main problem description with all the associated technical modeling assumptions is presented in Section II. The main technical results of this paper are then crisply summarized and their implications are discussed in Section III. Section IV describes the proposed constructive distributed coding and field reconstruction scheme and the analysis of MSE performance which leads to the technical results of Section III. For completeness, in Section IV-A we also briefly discuss sensor deployment issues but this is not the focus of this work. In Section V, we discuss the close connections between the work in [2], [3], and the present work, and establish the fundamental statistical and performance equivalence of the core techniques in these studies. We also discuss how the scenario of arbitrary unbounded noise and threshold distributions can be accommodated when the statistics are known. We conclude in Section VI by summarizing the main findings of this work. The proofs of two main results are presented in the appendices.

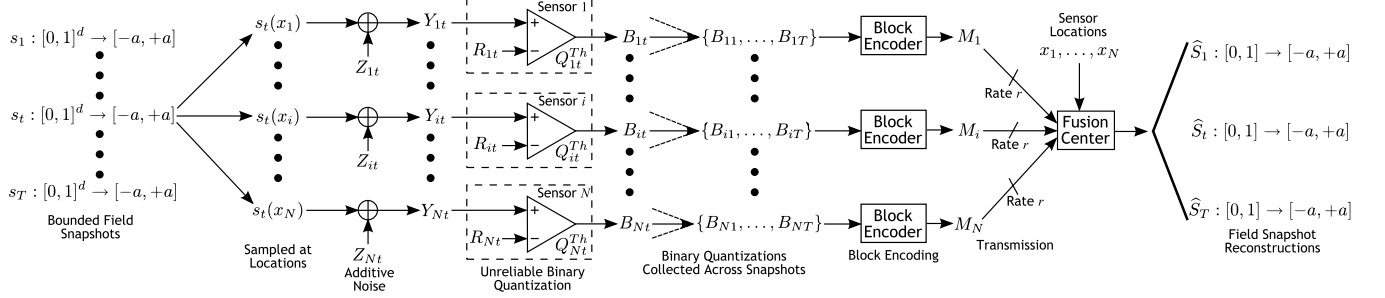


Fig. 1. **Block diagram of a distributed field reconstruction sensor-network using randomized 1-bit SQ with block-coding.** Sensor i quantizes its noisy observations, Y_{i1}, \dots, Y_{iT} , to the binary values B_{i1}, \dots, B_{iT} . The sensor then generates the message $M_i \in \{1, \dots, 2^{rT}\}$ based on these quantized values. These messages $\{M_i\}$ are then relayed to the fusion center where the field estimates \hat{S}_t are produced.

II. DISTRIBUTED FIELD RECONSTRUCTION SENSOR-NETWORK (DFRS) SETUP

A. Field Model

We consider a sequence of T discrete-time snapshots of a spatio-temporal field.³ Each snapshot is modeled as a continuous⁴ bounded function,

$$s_t : G \rightarrow \mathbb{R} : \forall x \in G, \forall t \in \{1, \dots, T\}, |s_t(x)| \leq a < +\infty,$$

where $G \subseteq \mathbb{R}^d$ is a known geographical region of interest in d -dimensional real space and a is a known bound on the maximum field dynamic range. Although the results of this paper hold for any G which is bounded and is the closure of its nonempty interior, for simplicity and clarity of exposition, we will assume $G = [0, 1]^d$, the d -dimensional unit-hypercube, in the sequel. Distances are measured with respect to a norm⁵ $\|\cdot\|$, which for this work will be assumed to be the Euclidean 2-norm. Since the fields are continuous functions on the compact set G , they are in fact uniformly continuous on G [22].

³If the spatio-temporal field is temporally bandlimited then the field values at intermediate time points can be interpolated from the estimates at discrete time snapshots if the temporal sampling rate is (strictly) higher than the temporal Nyquist rate of the field. The associated MSE will be no larger than the maximum MSE of the estimates across the discrete-time snapshots times a proportionality constant.

⁴More generally, our results can be extended to arbitrary, amplitude-bounded, measurable functions. For such functions the pointwise MSE bounds given in Section III-A still hold. The estimates at the points of continuity will have MSE tending to 0 as the network size scales. However, the points of discontinuity may have a finite, but non-zero MSE floor.

⁵For asymptotic results in which distance $\rightarrow 0$, any norm on \mathbb{R}^d would suffice since all norms on any finite-dimensional Banach space are equivalent [22, Theorem 23.6, p. 177].

Results on the fidelity of the field reconstruction will be described in terms of the local and global moduli of continuity associated with the field:

Definition 2.1: (Local modulus of continuity) The local modulus of continuity $\omega_t : [0, \infty) \times G \rightarrow [0, \infty)$ of the function $s_t(x)$ at the point $x \in G$ is defined as

$$\omega_t(\delta, x) \triangleq \sup_{\{x' \in G : \|x - x'\| \leq \delta\}} |s_t(x) - s_t(x')|.$$

Note that for all $x \in G$, $\omega_t(\delta, x)$ is a nondecreasing function of δ and that it $\rightarrow 0$ as $\delta \rightarrow 0$ since $s_t(x)$ is continuous at each point x in G .

Definition 2.2: (Global modulus of continuity) The global modulus of continuity $\tilde{\omega}_t : [0, \infty) \rightarrow [0, \infty)$ of the function $s_t(x)$ is defined as

$$\tilde{\omega}_t(\delta) \triangleq \sup_{x \in G} \omega_t(\delta, x).$$

Again note that $\tilde{\omega}_t(\delta)$ is a nondecreasing function of δ and that it $\rightarrow 0$ as $\delta \rightarrow 0$ since $s_t(x)$ is uniformly continuous over G .

The global and local moduli of continuity of a spatial field respectively reflect the degree of global and local spatial smoothness of the field with smaller values, for a fixed value of δ , corresponding to greater smoothness. For example, for a spatially constant field, that is, for all $x \in G$, $s_t(x) = s_t$ (a constant), we have $\tilde{\omega}_t(\delta) = 0$ for all $\delta \geq 0$. For $d = 1$ and fields with a uniformly bounded derivative, that is, for all $x \in G$, $\sup_{x \in G} |d(s_t(x))/dx| = \Delta < +\infty$, $\tilde{\omega}_t(\delta) \leq \Delta \cdot \delta$. More generally, for a Lipschitz- γ spatial function (see [1]) $s_t(x)$, we have $\tilde{\omega}_t(\delta) \propto \delta^\gamma$. Closed-form analytical expressions of moduli of continuity may not be available for arbitrary fields but bounds often are. Sometimes bounds that are tight in the limit as $\delta \rightarrow 0$ are also available. From Definitions 2.1, 2.2, and the boundedness of the field dynamic range, it also follows that for all $\delta \geq 0$, for all $x \in G$, and for all $t \in \{1, \dots, T\}$, we have

$$0 \leq \omega_t(\delta, x) \leq \tilde{\omega}_t(\delta) \leq 2a < +\infty.$$

B. Sensor Placement

We assume that we have a dense, noncooperative network of N sensors distributed uniformly over a hypercube partitioning of $G = [0, 1]^d$. The space $G = [0, 1]^d$ is uniformly partitioned into $L = l^d$ (where l is an integer) disjoint, hypercube supercells of side-length $(1/l)$. Each supercell is then further uniformly partitioned into $M = m^d$ (where m is an integer) hypercube subcells of side-length $(1/(lm))$, giving a total of LM subcells. In our distributed field coding and reconstruction scheme, described in Section IV, the field estimate for each snapshot is constant over each supercell and is formed by

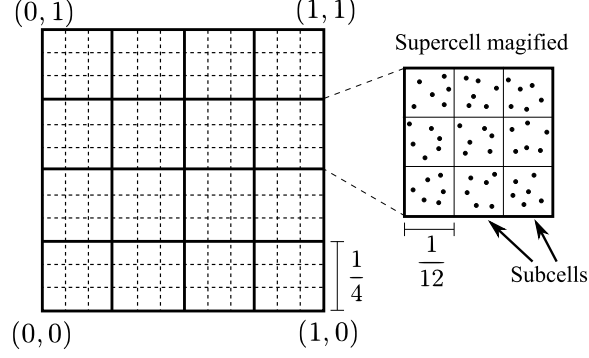


Fig. 2. **Example uniform sensor deployment and cell hierarchy over $[0, 1]^2$ ($d = 2$).** Here, $N = 864$ sensors are deployed over $L = 4^2$ supercells of side-length $(1/4)$ and $M = 3^2$ subcells per supercell of side-length $(1/(3 \cdot 4))$, resulting in 6 sensors per subcell.

averaging the measurements from a partial set of the sensors determined by the subcells. This field reconstruction scheme requires knowledge of the sensor locations only up to supercell (not subcell) membership. Therefore, it has some natural robustness against sensor location uncertainty or error. The significance of the super and subcells will become clear in the sequel (Sections III and IV).

We assume that the sensor deployment mechanism is able to uniformly distribute the sensors over the subcells. We define this uniform sensor deployment condition with:

Definition 2.3: (Uniform sensor deployment) We say that a sensor deployment method is uniform if exactly $n \triangleq (N/(LM))$ sensors are located in each subcell.

Definition 2.3 describes ideal sensor deployment conditions and can be achieved by locating the sensors over a uniform grid. However, precise control of sensor locations may not be possible in practice. Since we are not primarily concerned about the details of deployment, we defer discussion of such issues to Section IV-A, where we introduce a stochastic deployment model in order to capture the uncertainty of realistic deployment mechanisms. In Section IV-A, we show that this deployment method satisfies a relaxed version of Definition 2.3, the asymptotic nearly uniform deployment condition given by Definition 4.1, which does not significantly change the estimator performance.

For clarity of presentation, we will assume that the deployment scheme being used satisfies the uniform sensor deployment condition given in Definition 2.3. We also assume that each sensor is aware of which subcell it is in. Figure 2 illustrates the cell hierarchy and an example sensor deployment for the $d = 2$ dimensional case.

C. Sensor Observation and Coding Models

1) *Sensor Observation Noise*: The sensor observations are corrupted by bounded, zero-mean additive noise which is independent across sensors, but can be arbitrarily correlated across field snapshots⁶. Let Z_{it} denote the noise affecting the observation of the t^{th} snapshot by the i^{th} sensor, and define the $\mathbf{Z} \triangleq \{Z_{it}\}_{i=1, t=1}^{N, T}$ (the collection of all of the noise random variables) and $\mathbf{Z}_i \triangleq \{Z_{it}\}_{t=1}^T$ (the collection of all of the noise random variables for a given sensor i). The noise \mathbf{Z} has an unknown joint cumulative distribution function (cdf) $F_{\mathbf{Z}}(\mathbf{z})$ that can be arbitrary within the zero-mean, boundedness and independence constraints already stated. The maximum dynamic range of the noise $b \in [0, +\infty)$ is known. The noisy observation of field snapshot $t \in \{1, \dots, T\}$ made by sensor $i \in \{1, \dots, N\}$ is given by

$$Y_{it} = s_t(x_i) + Z_{it},$$

where x_i is the location of the i^{th} sensor and $\mathbf{Z} \sim \text{cdf } F_{\mathbf{Z}}(\mathbf{z})$. We use \mathcal{F} to denote the set of all joint cdfs that are factorizable into N zero-mean joint cdfs on \mathbb{R}^T with support within $[-b, +b]^T$, that is, $F_{\mathbf{Z}}(\mathbf{z}) = \prod_{i=1}^N F_{\mathbf{Z}_i}(\mathbf{z}_i)$ where $F_{\mathbf{Z}_i}(\mathbf{z}_i)$ is a zero-mean joint cdf (corresponding to the noise random variables for sensor i) with support within $[-b, +b]^T$. Note that \mathcal{F} captures the feasible set of joint noise cdfs for the bounded-amplitude, zero-mean, and independence assumptions. Also note that $|Y_{it}| \leq |s_t(x_i)| + |Z_{it}| \leq c \triangleq (a + b)$.

2) *Randomized 1-bit SQ with Block Coding*: Due to severe precision and reliability limitations, each sensor $i \in \{1, \dots, N\}$, has access to only to a vector of unreliable binary quantized samples $\mathbf{B}_i \triangleq (B_{i1}, \dots, B_{iT})$ for processing and coding and not direct access to the real-valued noisy observations Y_{i1}, \dots, Y_{iT} . The quantized binary sample B_{it} is generated from the corresponding noisy observation Y_{it} through a randomized mapping $Q_{it} : [-c, c] \rightarrow \{0, 1\}$: for each $i \in \{1, \dots, N\}$ and each $t \in \{1, \dots, T\}$,

$$B_{it} = Q_{it}(Y_{it}),$$

where we assume that the mappings Q_{it} are independent across sensors i , but can be arbitrarily correlated across snapshots t . We denote the conditional marginal statistics of the quantized samples by $p_{B_{it}|Y_{it}}(y) \triangleq \mathbb{P}(B_{it} = 1 | Y_{it} = y)$. We are specifically interested in cases where $p_{B_{it}|Y_{it}}(y)$ is an affine function of y since it allows estimates of the fields to be made from the B_{it} 's without knowledge of the noise distribution (see Appendix I). Specifically we consider the conditional distribution

$$p_{B_{it}|Y_{it}}(y) = \left(\frac{y + c}{2c} \right).$$

⁶The measurement snapshot timers of all the participating sensors are assumed to be synchronized.

This conditional distribution can be achieved by a quantization method which is based on comparing the noisy observation with a random uniformly distributed threshold given by

$$B_{it} = Q_{it}^{Th}(Y_{it}) \triangleq \mathbf{1}(Y_{it} > R_{it}), \quad (2.1)$$

where the R_{it} 's are $\text{Unif}[-c, c]$ random thresholds which are independent across sensors i , but arbitrarily correlated across snapshots t , and $\mathbf{1}(\cdot)$ denotes the indicator function:

$$\mathbf{1}(Y_{it} > R_{it}) = \begin{cases} 1 & \text{if } Y_{it} > R_{it}, \\ 0 & \text{otherwise.} \end{cases}$$

This uniform random-threshold 1-bit SQ model partially accounts for some practical scenarios that include (i) comparators with a floating threshold voltage, (ii) substantial variation of preset comparator thresholds accompanying the mass-manufacture of low-precision sensors, (iii) significant environmental fluctuations that affect the precision of the comparator hardware, or generally (iv) unreliable comparators with considerable sensing noise and jitter. An alternative justification is that the random thresholds are intentionally inserted as a random dither. Scenario (i) can be accommodated by independence across snapshots, scenario (ii) can be accommodated by complete correlation (fixed) across snapshots, and scenarios (iii) and (iv) can be accommodated by arbitrary correlation across snapshots.

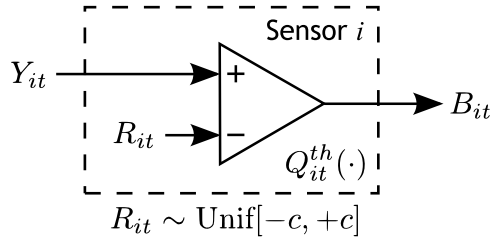


Fig. 3. **Quantizer hardware example.** The sensing model described by the $Q_{it}^{Th}(\cdot)$ function in (2.1) can be implemented by a comparator with a uniformly distributed threshold. These thresholds are independent across sensors, but arbitrarily correlated across snapshots, allowing many scenarios to be accommodated.

Each sensor i utilizes a block encoder to “compress” its vector of T quantized samples \mathbf{B}_i to a message $M_i \in \{1, 2, \dots, 2^{rT}\}$ before transmitting to the fusion center. The block encoder and message for sensor i are given by

$$f_i : \{0, 1\}^T \rightarrow \{1, 2, \dots, 2^{rT}\}, \quad M_i = f_i(B_{i1}, \dots, B_{iT}),$$

where r is the coding rate in bits per sensor per snapshot. For $r \geq 1$ compression is trivial since \mathbf{B}_i can assume no more than 2^T distinct values which can be indexed using T bits.

D. Transmission and Field Reconstruction

In this work, a data fusion center is any point of data aggregation and/or processing in the sensor network and can be real or virtual. For instance, sensors can be dynamically organized into clusters with different sensors assuming the role of a fusion center at different times [23]. To conform with the existing base of digital communication architectures, our problem setup abstracts the underlying transmission network of sensors effectively as a network of bit pipes. These bit pipes are capable of reliably delivering these N messages (the payloads) and the network addresses of the message origination nodes (the headers) to the fusion center. This enables the fusion center to correctly associate the spatial location information with the corresponding sensor field-measurement information for reliable field reconstruction. In practice, sensor data can be moved to the fusion center through a variety of physical-layer transport mechanisms, example, a stationary base-station with directional antenna arrays, a mobile data collector, and passive sensor querying mechanisms involving, for instance, laser-beams and modulating mirrors [24].

Separating the distributed field reconstruction problem into efficient data acquisition and efficient data transport parts through a finite-rate reliable bit-pipe abstraction may be suboptimal [25, p. 449], [15], [16]. For instance, in some scenarios multihop communication is not needed and the characteristics of the field, the communication channel, and the distortion-metric are “matched” to one another. In such a scenario, uncoded “analog” transmission can offer huge performance gains if the synchronization of sensor transmissions can be orchestrated at the physical layer to achieve beamforming gains and the network channel state information is available to the transmitting sensors [15]. Certain aspects of this analog transmission can be incorporated within our field reconstruction framework and is briefly discussed in the remark just before Section IV-A.

For our reconstruction scheme, described in Section IV, the fusion center only needs to be able to spatially localize the origin of each message to within the supercell resolution. This can be achieved by having each sensor append a $\log(LM)$ bits long label to its message. This results in a total sensor-location rate-overhead of $r_{ohd} = (N/T) \log(LM)$ bits per snapshot on the network information transport costs. This overhead will be negligible if $T \gg N \log(LM)$. If the underlying sequence of fields are spatially constant, then, the sensor location information is not needed at the fusion center (see Corollary 3.1 and Section IV).

The fusion center forms the estimates of the T fields based on the sensor messages using the reconstruction functions

$$g_t : G \times \{1, 2, \dots, 2^{rT}\}^N \rightarrow [-a, a], \quad \forall t \in \{1, \dots, T\}.$$

The estimate of field t at point $x \in G$ is denoted by

$$\hat{S}_t(x) = g_t(x, M_1, \dots, M_N).$$

Definition 2.4: (Rate- r DFRS) A rate- r DFRS based on randomized 1-bit SQ with block coding is defined by the set of rate- r encoder functions $\{f_i(\cdot)\}_{i=1}^N$ and the set of reconstruction functions $\{g_t(\cdot)\}_{t=1}^T$.

Figure 1 depicts a rate- r DFRS using randomized 1-bit SQ with block coding.

1) *Performance Criterion:*

Definition 2.5: (Pointwise MSE) The pointwise MSE of the estimate of field t at location $x \in G$, for a given rate- r DFRS and a specific noise joint cdf $F_{\mathbf{Z}}(\mathbf{z}) \in \mathcal{F}$, is given by

$$D_t(x; F_{\mathbf{Z}}) = \mathbb{E}[(\hat{S}_t(x) - s_t(x))^2].$$

Since we are interested in schemes that will work for *any* noise cdf in \mathcal{F} , we consider the worst-case $D_t(x; F_{\mathbf{Z}})$ over all possible $F_{\mathbf{Z}} \in \mathcal{F}$. We also consider the maximization over all fields and all locations in G since we want to reconstruct every point of every field with high fidelity.

Definition 2.6: (Worst-case MSE) The worst-case MSE D is given by

$$D = \max_{t \in \{1, \dots, T\}} \sup_{x \in G} \sup_{F_{\mathbf{Z}} \in \mathcal{F}} D_t(x; F_{\mathbf{Z}}).$$

Our objective is to understand the scaling behavior of MSE with N , T , and r . The next section summarizes our partial results in this direction.

III. MAIN RESULTS

A. Achievable MSE Performance

Our first result gives an upper bound on the MSE achievable through a constructive DFRS based on randomized 1-bit SQ with block coding for rate $r = 1/M$, where M is the number of subcells per supercell. The actual scheme will be described in Section IV. The MSE analysis appears within the proof of the theorem detailed in Appendix I. This achievable MSE upper bound can be made to decrease to zero as sensor-density goes to infinity (see (3.1)) without knowledge of the local or global smoothness properties of the sequence of fields. Furthermore, this scheme is universal in the sense that it does not assume knowledge of $F_{\mathbf{Z}}(\mathbf{z})$ beyond membership to \mathcal{F} .

Theorem 3.1: (Achievable MSE performance: Randomized 1-bit SQ and $r = 1/M$) There exists a rate- $r = 1/M$ DFRS based on randomized 1-bit SQ with block coding (e.g., the scheme of Section IV)

such that for all $x \in G$, $t \in \{1, \dots, T\}$, and $F_{\mathbf{Z}}(\mathbf{z}) \in \mathcal{F}$,

$$\begin{aligned} D_t(x; F_{\mathbf{Z}}) &\leq \omega_t^2 \left(\frac{\sqrt{d}}{\sqrt[d]{L}}, x \right) + \left(\frac{LMc^2}{N} \right) \\ &\leq \tilde{\omega}_t^2 \left(\frac{\sqrt{d}}{\sqrt[d]{L}} \right) + \left(\frac{LMc^2}{N} \right). \end{aligned}$$

Proof: See Section IV and Appendix I. ■

Note that Theorem 3.1 holds for arbitrary fields. The modulus of continuity terms in the local (first) and global (second) upper bounds of Theorem 3.1 are due to the bias of the field estimates and the $\left(\frac{LMc^2}{N} \right)$ term is due to the variance of the field estimates (see (4.2) in Section IV). From Theorem 3.1 and the properties of moduli of continuity (see Section II-A), it follows that for the coding and reconstruction scheme of Section IV, as $N \rightarrow \infty$, the estimate $\hat{S}_t(x)$ uniformly converges, in a mean square sense, to $s_t(x)$ for all $x \in G$, provided that

$$(i) \left(\frac{N}{L} \right) \rightarrow \infty, \text{ and } (ii) L \rightarrow \infty. \quad (3.1)$$

It also follows that the worst-case MSE scaling behavior (see Definition 2.6) is bounded by

$$D \leq \max_{t \in \{1, \dots, T\}} \left\{ \tilde{\omega}_t^2 \left(\frac{\sqrt{d}}{\sqrt[d]{L}} \right) + \left(\frac{LMc^2}{N} \right) \right\} \quad (3.2)$$

and that $D \rightarrow 0$ as N and L scale as in (3.1).

Implications: These results allow us to make the per sensor per snapshot bit rate r , worst-case MSE D , and sensor message ID overheads (given by $(N/T) \log(LM)$ bits) simultaneously smaller than any arbitrarily small desired values r^* , D^* , $\epsilon > 0$, respectively. First, we can choose a sufficiently large number of subcells per supercell M^* such that the rate $r = 1/M^* < r^*$. Then we can choose a sufficiently large number of sensors N^* and number of supercells L^* such that the bound on D given by (3.2) is made less than D^* . Note that both N^* and M^* can be further increased while keeping the ratio M^*/N^* fixed without changing the bound on D . This corresponds to increasing the total number of sensors N , decreasing the per sensor rate $r = 1/M$, but keeping the total network per snapshot rate $Nr = N/M$ and distortion D fixed. Finally, we can look at a sufficiently large number of snapshots T^* such that network message overheads $(N^*/T^*) \log(L^*M^*) < \epsilon$.

In the constructive coding and field reconstruction scheme of Section IV, the field estimates are piecewise constant over the supercells. The estimate in each supercell is formed from only $n = (N/(LM))$ of the $Mn = (N/L)$ quantized observed values coming from the sensors located in that supercell. Since only $(1/M)$ of the total available quantized observed values for each snapshot are used, the transmission rate of $(1/M)$ is achievable by indexing only the necessary values (see Section IV for details). As the

number of supercells L increases, the piecewise constant estimate becomes finer and the bias is decreased. Also, as the number of sensors per supercell is increased, more observations are used thus decreasing the variance of the estimate.

Since the variance term $\frac{LMc^2}{N}$ in the upper bound of Theorem 3.1 can decrease no faster than $O(1/N)$, the decay of the global MSE upper bound, in the proposed constructive scheme, can be no faster than $O(1/N)$. However, the decay rate of $\frac{LMc^2}{N}$ is hindered by the fact that L simultaneously needs to approach infinity for the bias term $\tilde{\omega}_t^2\left(\frac{\sqrt{d}}{\sqrt[4]{L}}\right)$ to decay to 0. When $\tilde{\omega}_t(\cdot)$ is not identically zero, a bias–variance tradeoff exists and the appropriate relative growth rate for L with N that minimizes the decay rate of the global MSE upper bound of Theorem 3.1 is determined by the following condition

$$\tilde{\omega}_t^2\left(\frac{\sqrt{d}}{\sqrt[4]{L}}\right) = \Theta\left(\frac{L}{N}\right).$$

For certain classes of signals for which the global modulus of continuity has a closed form, the optimum growth rate can be explicitly determined. For instance, if $d = 1$ and $\tilde{\omega}_t(\delta) = \Delta \cdot \delta$ (Lipschitz–1 fields), $L_{opt}(N) = \Theta(N^{1/3})$ for which $MSE = O(N^{-2/3})$.

Corollary 3.1: (Achievable MSE performance: Randomized 1-bit SQ, $r = 1/M$, and constant fields) If for all $x \in G$ and all $t \in \{1, \dots, T\}$, we have $s_t(x) = s_t$, or equivalently, for all $\delta \geq 0$ and all $t \in \{1, \dots, T\}$, $\tilde{\omega}_t(\delta) = 0$, then the result given by (3.2) reduces to

$$D \leq \left(\frac{Mc^2}{N}\right),$$

where we can set $L = 1$ to minimize the bound.

Only $L = 1$ supercell is needed for an accurate piecewise constant reconstruction of a constant field. Furthermore, all snapshot–estimates given by the scheme from Section IV are unbiased in this case. Also, the spatial locations of sensors are irrelevant: the MSE behavior is governed purely by the number of sensors N regardless of how they are distributed over the subcells. The N sensors must still be uniformly assigned to one of M groups (for the purpose of transmission coordination to achieve the compression factor of $1/M$), however these groups need not have any geographical significance.

The MSE results given by Theorem 3.1 show that the field snapshot estimates converge uniformly in MSE and upper bound the MSE decay rate. Every point of every estimate, in fact, converges almost surely to the true value. We also state a central limit theorem (CLT) result regarding the estimation error.

Theorem 3.2: (Almost–sure convergence of field estimates) There exists a rate- $r = 1/M$ DFRS based on randomized 1-bit SQ with block coding (described in Section IV) such that for all $x \in G$, $t \in$

$\{1, \dots, T\}$, and $F_{\mathbf{Z}}(\mathbf{z}) \in \mathcal{F}$,

$$\widehat{S}_t(x) \xrightarrow{\text{a.s.}} s_t(x),$$

as N and L scale as given in (3.1).

Proof: See Section IV and Appendix II. ■

Corollary 3.2: (Central limit theorem for estimation errors) For the rate $r = 1/M$ DFRS of Section IV, the normalized error at point $x \in G$ for the estimate of field snapshot $t \in \{1, \dots, T\}$, given by

$$\frac{\widehat{S}_t(x) - s_t(x)}{\sqrt{\text{var}[\widehat{S}_t(x) - s_t(x)]}},$$

is asymptotically zero-mean, unit-variance, normal as N and L scale as given in (3.1), for any $F_{\mathbf{Z}}(\mathbf{z}) \in \mathcal{F}$.

Proof: The proof is similar to and follows directly from the proof of Theorem 2.4 in [2]. ■

B. Order-Optimal Minimax MSE for Constant Fields

The minimax reconstruction MSE over the class of constant fields is given by

$$\inf_{\{g_t\}_{t=1}^{t=T}} \sup_{F_{\mathbf{Z}} \in \mathcal{F}, s_t \in \mathcal{S}} D,$$

where the infimum is taken over all possible estimators and the supremum is taken over all noise distributions and fields from the class of constant fields which is denoted by \mathcal{S} . The achievable MSE result given by Corollary 3.1 establishes an upper bound on the minimax reconstruction MSE. Theorem 3.3 lower bounds the minimax reconstruction MSE for any rate r DFRS that produces unbiased estimates for the case of spatially constant fields.

Theorem 3.3: (Lower bound on MSE: Unbiased estimators for constant fields) For a sequence of spatially constant fields and any DFRS which produces unbiased field estimates, there exists a joint cdf $F_{\mathbf{Z}} \in \mathcal{F}$ such that for noise distributed according to $F_{\mathbf{Z}}$ the MSE is lower bounded by

$$\mathbb{E}[(\widehat{S}_t - s_t)^2] \geq \left(\frac{C_t}{N}\right), \quad \text{for all } t \in \{1, \dots, T\},$$

where C_t is finite, non-zero, and does not depend on N . Therefore,

$$\inf_{\{g_t\}_{t=1}^{t=T}} \sup_{F_{\mathbf{Z}} \in \mathcal{F}, s_t \in \mathcal{S}} D \geq \max_{t \in \{1, \dots, T\}} \left(\frac{C_t}{N}\right).$$

Proof: Since $\{s_t\} \rightarrow \{Y_{it}\} \rightarrow \{B_{it}\} \rightarrow \{M_i\}$ forms a Markov chain, the estimates based on the sensor messages $\{M_1, \dots, M_N\}$ cannot have a lower MSE than estimates based on the noisy observations $\{Y_{it}\}$. Let $F_{\mathbf{Z}} \in \mathcal{F}$ be any well-behaved, non-trivial, joint cdf such that the Z_{it} are iid and the conditional probabilities of Y_{it} given the fields satisfy the regularity conditions necessary for the Cramér-Rao bound

[26] to be applied. By the Cramér–Rao bound, the MSE of each field estimate based on $\{Y_{it}\}$ is lower bounded by $\frac{C_t}{N}$ where C_t is finite, non-zero, and depends on F_Z , but does not depend on N . Note that the bound also applies to general randomized 1-bit SQ functions $Q_{it}(\cdot)$ including those based on uniform random thresholds $Q_{it}^{Th}(\cdot)$ (see (2.1)). ■

Combining the results of Corollary 3.1 and Theorem 3.3 establishes that the order-optimal minimax MSE for spatially constant fields is $\Theta(1/N)$ and that the scheme of Section IV achieves this order optimal performance.

IV. PROPOSED CONSTRUCTIVE DISTRIBUTED CODING AND FIELD RECONSTRUCTION SCHEME

In this section we present the proposed DFRS scheme that was alluded to in Section III. In this scheme, sensors create the quantized binary samples $\{B_{it}\}$ from their observations $\{Y_{it}\}$ through comparisons with the random thresholds $\{R_{it}\}$, as described in (2.1) of Section II-C.2. The field estimates are piecewise constant over the supercells, where the estimate formed in each supercell is a function of only $(N/(LM))$ of the (N/L) quantized observed values coming from the sensors located in that supercell. This allows fractional transmission rates of $r = 1/M$ through a simple time-sharing based compression method. Note that there can be uncertainty in the sensor locations, within a degree given by the size of a supercell, at the fusion center, since it is only necessary for the fusion center to know which supercell each sensor is located in.

Each sensor i , instead of transmitting all of its T bits (the vector of its binary quantized observations $\mathbf{B}_i = (B_{i1}, \dots, B_{iT})$), transmits only $rT = T/M$ of them and the remaining observations are dropped. Or alternatively, the sensor may sleep and not record the remaining measurements. The two-level hierarchy of supercells and subcells described in Section II-B is used in order to properly determine which bits sensors should drop or keep. Within each supercell, each sensor i from subcell $k \in \{1, \dots, M\}$ communicates only every M^{th} bit (offset by k), that is $\{B_{i,k+Ml}\}_{l=0}^{l=(T/M)-1}$. These rT bits can be uniquely represented by the message $M_i \in \{1, \dots, 2^{rT}\}$ and losslessly communicated to the fusion center. Thus for snapshot $t \in \{1, \dots, T\}$, only the bits from sensors in the $[(t-1) \bmod M + 1]^{\text{th}}$ subcell of each supercell are communicated to the fusion center. The set of all sensor indices corresponding to the $n = (N/(LM))$ sensors belonging to the $[(t-1) \bmod M + 1]^{\text{th}}$ subcell of supercell j will be denoted by $I(j, t)$. In other words, this set of indices corresponds to all those sensors which are located in supercell j and are responsible for recording and encoding a bit in the t -th snapshot.

For notational simplicity, the reconstruction function $\hat{S}_t(x) = g_t(x, M_1, \dots, M_N)$ will be described

directly in terms of the available binary quantized observations B_{it} ⁷ and not the encoded messages $\{M_i\}$ which are information equivalent. The reconstruction function $\hat{S}_t(x)$ is piecewise constant and is described as follows. The field $s_t(x)$ is reconstructed as a constant over each supercell j . The constant estimate is given by

$$\hat{S}_{tj} \triangleq 2c \left[\frac{1}{n} \sum_{i \in I(j,t)} B_{it} \right] - c, \quad (4.1)$$

which is the simple average (shifted and scaled into $[-c, +c]$) of the available quantized binary observations of snapshot t from sensors located in supercell j . The overall piecewise-constant estimate for $s_t(x)$ can be then described as

$$\begin{aligned} \hat{S}_t(x) &= g_t(x, M_1, \dots, M_N) \\ &\triangleq \sum_{j=1}^L \hat{S}_{tj} \mathbf{1}(x \in \mathcal{X}_j), \end{aligned} \quad (4.2)$$

where $\mathcal{X}_j \subseteq [0, 1]^d$ is the set of points within the j^{th} hypercube supercell and $\mathbf{1}(x \in \mathcal{X}_j)$ given by

$$\mathbf{1}(x \in \mathcal{X}_j) = \begin{cases} 1 & \text{if } x \in \mathcal{X}_j, \\ 0 & \text{otherwise,} \end{cases}$$

is the indicator function of the set \mathcal{X}_j . Other more sophisticated reconstruction algorithms are possible. For instance, instead of the simple average used in (4.1), one may use a weighted average with convex weights, and for the overall reconstruction in (4.2), one may use a piecewise-linear or other higher-order interpolation algorithms such as those based on cubic B-splines (see [2]). The resulting MSE will be of the same order. We use the former (simple average, piecewise-constant) reconstruction because its description and analysis is more compact. Appendix I proves that the MSE of this constructive coding and reconstruction scheme is upper bounded by the result described in Theorem 3.1.

Remark: As discussed at the beginning of Section II-D, physical-layer network data transport issues are not the focus of this work. However, if synchronized analog beamforming from the sensors within each subcell to the fusion center can be achieved, then the summation in the reconstruction given by equation (4.1) can be realized directly in the analog physical layer, by “adding signals in the air”, using a simple binary pulse amplitude modulation signaling scheme at each sensor. The additional estimation error variance due to the receiver amplifier noise at the fusion center will decrease as $1/n$ by scaling the sampled received waveform by $1/n$ as in (4.1). This will lead to corresponding achievable power versus distortion tradeoffs (as opposed to bits versus MSE or sensors versus MSE) which can be quantified.

⁷The set of binary quantized observations for snapshot t which are available at the fusion center is given by $\{B_{it}\}_{\{i \in \cup_{j=1}^L I(j,t)\}}$

A. Sensor Deployment Considerations

The conditions given by Definition 2.3 correspond to exactly $(N/(LM))$ sensors uniformly falling into each subcell with probability one for all N , L , and M (ignoring integer affects). In the regime of perfect sensor placement control (or when placement error is negligible compared to the width of the cells), this condition is trivially realized by locating the sensors on a uniform grid. However, such precise sensor placement control might not be achievable in practice. In order to address this issue we introduce a stochastic sensor deployment model, one that captures an extreme case of (uncontrollable) sensor placement uncertainty where each sensor is deployed according to a uniform distribution over $[0, 1]^d$. We also relax the uniform sensor placement to an asymptotic nearly uniform sensor deployment given by Definition 4.1.

Definition 4.1: (Asymptotic nearly uniform sensor deployment) We say that a sensor deployment method is asymptotically nearly uniform with parameters (γ, ϵ, N^*) if at least $\gamma n \triangleq \gamma(N/(LM))$ are located in each subcell with probability at least $1 - \epsilon$ for all $N > N^*$, where $\gamma \in (0, 1]$ represents the inverse of the “over-provisioning” factor for the number of sensors needed to be deployed.

This relaxation does not significantly impact our results since we are interested in the asymptotic results (as L and N scale as in (3.1)) where the γ and ϵ parameters of Definition 4.1 can be made negligible. Our stochastic deployment scheme satisfies this asymptotic nearly uniform condition given in Definition 4.1, and also almost surely satisfies the uniform deployment condition given by Definition 2.3 for $N \rightarrow \infty$.

Consider the scenario where N sensors are deployed iid and uniformly over $G = [0, 1]^d$. The corresponding indices of the subcells (the total LM subcells can be indexed by an integer from 1 to LM) that the N sensors fall is denoted by the random sequence $\mathbf{J} = (J_1, \dots, J_N)$. Here, $J_i \sim \text{iid } U$, where $U \triangleq (1/(LM), \dots, 1/(LM))$ is the uniform probability mass function over LM discrete values. We examine the N -type (empirical distribution) $P_{\mathbf{J}}^{(N)}$ of \mathbf{J} in order to examine the level of uniformity in the sensor deployment. An empirical distribution equal to U corresponds to the uniform deployment condition of Definition 2.3 being met. Since the indices are also distributed iid according to U , by the strong law of large numbers, the empirical distribution converges almost surely to U as $N \rightarrow \infty$, and thus almost surely the sensors will be deployed uniformly over the subcells according to Definition 2.3 as $N \rightarrow \infty$.

Also, a result from large deviations theory bounds the probability that the empirical distribution will not be in a δ -neighborhood of the uniform distribution. This corresponds to the event where there exists a subcell that has more than $\frac{N(1+\delta)}{LM}$ or fewer than $\frac{N(1-\delta)}{LM}$ sensors located within it. Let \mathcal{P}^N be the set of

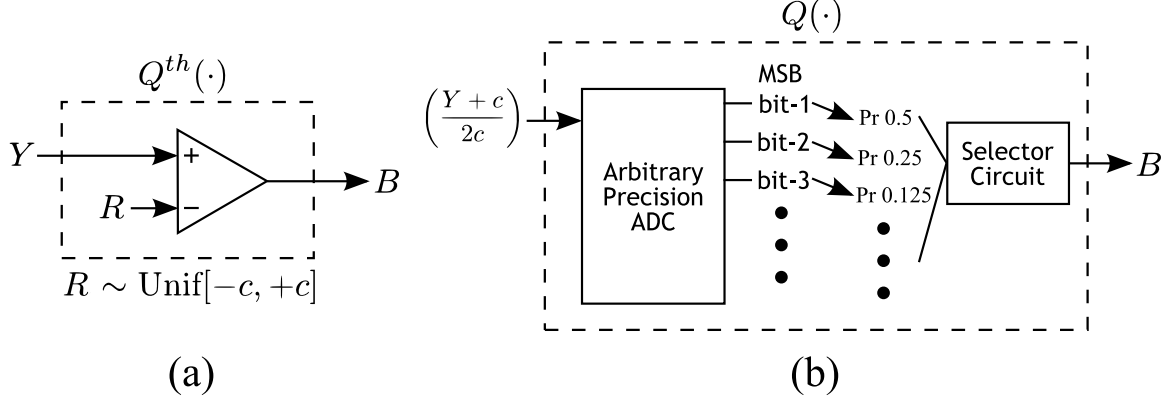


Fig. 4. The $Q_{it}^{Th}(\cdot)$ function in (2.1) and the $Q(\cdot)$ function of [3] suggest markedly different hardware implementations. The former naturally suggests (a), where the binary quantized value is produced by a simple comparison to a random threshold X . The latter suggests (b), where an arbitrarily-precise ADC circuitry probabilistically selects an arbitrary bit of the observed value. Interestingly, these two implementations produce statistically equivalent quantized outputs B given identical inputs Y .

N -dimensional probability distributions, $U^\delta \triangleq [(1-\delta)/(LM), (1+\delta)/(LM)]^N$ be the δ -neighborhood around the uniform probability mass function U , $D(\cdot\|\cdot)$ denote the Kullback–Leibler distance [25], and

$$P^* = \arg \min_{P \in \mathcal{P}^N \setminus U^\delta} D(P\|U)$$

denote the probability distribution not in U^δ that is closest to U in Kullback–Leibler distance. It should be noted that $D(P^*\|U) > 0$ for all $\delta > 0$. Then by Sanov’s theorem [25, p. 292],

$$\begin{aligned} \mathbb{P}(P_J^N \in \mathcal{P}^N \setminus U^\delta) &\leq (N+1)^{LM} 2^{-ND(P^*\|U)} \\ &= 2^{-N(D(P^*\|U) - \frac{LM}{N} \log(N+1))}. \end{aligned} \quad (4.3)$$

This inequality bounds the probability that not all subcells have at least $\frac{N(1-\delta)}{LM}$ sensors within them. This shows that as long as the number of sensors deployed N grows faster than the actual number of sensors needed LM , then the near uniform deployment condition will be eventually met. Thus, this determines how many total sensors $N^* > LM$ need to be deployed in order to satisfy the asymptotic nearly uniform sampling condition of Definition 4.1 for a given desired ϵ and for $\gamma = 1 - \delta$.

V. DISCUSSION OF RELATED ONE-BIT ESTIMATION PROBLEMS AND EXTENSIONS

This section discusses the connections between the methods and results in [2], [3], and the present work. It is shown that the apparently different randomized 1-bit field estimation schemes in these studies are in fact statistically and MSE performance equivalent. We also address how, in the scenario of known noise

statistics, unbounded noise distributions and arbitrary threshold distributions can be accommodated. The general framework of the present work integrates the desirable field sensing and reconstruction properties and insights of the earlier studies and provides a unified view of the problem that simultaneously considers unreliable binary quantization, unknown arbitrary noise distributions, multiple snapshots of a temporally and spatially varying field, and communication rate issues. Since the work in both [2] and [3] deal with the reconstruction of only a single snapshot ($T = 1$), we will drop the snapshot indices t in our discussion to aid comparison.

A. One-Bit Randomized-Dithering

The problem setup of [2] may be viewed as the reconstruction of a single snapshot ($T = 1$) of a bounded, one-dimensional field ($d = 1$) from noiseless samples ($Z_i = 0$) at uniformly spaced (deterministic) sampling locations ($x_i = i/N$). In [2] the noiseless observations are binary quantized using random thresholds R_i s that have a known general distribution which satisfies certain technical conditions described in [2, Section II.A]. These technical conditions include the uniform distribution (considered in this paper) as a special case. An important conceptual difference is that in [2] the sensor quantization noise is viewed as a randomized dither signal which is intentionally added to the observations and that the dither cdf is known (it need not be uniform). The reconstruction explicitly exploits the knowledge of the dither statistics. Specifically, the noiseless observation Y_i , at sensor i , and the corresponding quantized binary sample B_i become

$$\begin{aligned} Y_i &= s(x_i), \\ B_i &= Q(Y_i) \triangleq \text{sgn}(Y_i + X_i), \end{aligned}$$

where X_i is iid dithering noise with a known distribution $p_X(\cdot)$ which satisfies certain technical assumptions as given in [2, Section II.A]. Note that taking the sign of the sum of the observation and random dither X_i is equivalent to comparing with the threshold $-X_i$. Thus the quantization function $Q(\cdot)$ of [2] is equivalent⁸ to a comparator with a random threshold that is distributed according to $p_X(-x)$. The quantization function $Q_{it}^{Th}(\cdot)$ in (2.1) can be viewed as a special case of this where $p_X(-x)$ is the uniform distribution over $[-c, c]$. The constructive scheme of Section IV and the analysis of this work shows that $Q_{it}^{Th}(\cdot)$ can in fact be used even on noisy field observations with an additive noise of *unknown* distribution.

⁸The sign function maps to $\{-1, +1\}$ whereas a threshold comparator maps to $\{0, 1\}$. However, the replacement of the -1 symbol with the 0 symbol is unimportant from an estimation viewpoint.

B. Parameter Estimation with One-Bit Messages

The parameter estimation problem in [3] corresponds to the special case of a spatially constant field ($s(x_i) = s$ for all i where the index t is omitted since $T = 1$) which is addressed by Corollary 3.1. We summarize below the key features of the randomized binary quantizer proposed in [3] and show that the randomized 1-bit SQ function $Q(\cdot)$ of [3] is statistically and MSE performance-wise equivalent to the uniform random threshold quantizer $Q_{it}^{Th}(\cdot)$ in (2.1). However, the $Q(\cdot)$ function of [3] implicitly requires sensors of arbitrarily high precision, a property that is undesirable for sensor hardware implementations.

In [3], each sensor i first shifts and scales its observation Y_i into interval $[0, 1]$ creating the value $\tilde{Y}_i \triangleq (\frac{Y_i + c}{2c})$. Next, each sensor i generates an auxiliary random variable α_i , which is iid across sensors and is geometrically distributed over the set of all positive integers: $\mathbb{P}(\alpha_i = j) = 2^{-j}$ for all $j \in \{1, 2, 3, \dots, \infty\}$. The final quantized binary sample B_i reported by sensor i is given by the α_i^{th} bit in the binary expansion of \tilde{Y}_i :

$$B_i = Q(Y_i) \triangleq B(\tilde{Y}_i, \alpha_i),$$

$$\text{where } \tilde{Y}_i = \sum_{j=1}^{\infty} B(\tilde{Y}_i, j) 2^{-j}. \quad (5.1)$$

Here, $B(\tilde{Y}_i, j)$ denotes the j^{th} bit of \tilde{Y}_i . For example, if $\tilde{Y}_i = 0.375$, then the first four bits of its binary expansion are given by $B(\tilde{Y}_i, 1) = 0$, $B(\tilde{Y}_i, 2) = 1$, $B(\tilde{Y}_i, 3) = 1$, and $B(\tilde{Y}_i, 4) = 0$. If $\alpha_i = 3$, then sensor i reports $B_i = 1$. This method for generating binary sensor messages requires sensors to have the operational ability to quantize an observed real number (the normalized values \tilde{Y}_i) to an arbitrarily high bit-resolution. Note that the binary values B_i are iid across all sensors and that its expected value is given by

$$\begin{aligned} \mathbb{E}[B_i] &= \mathbb{E}_{\tilde{Y}_i}[\mathbb{E}_{B_i}[B_i | \tilde{Y}_i]] \\ &= \mathbb{E}_{\tilde{Y}_i} \left[\sum_{j=1}^{\infty} B(\tilde{Y}_i, j) 2^{-j} \right] \\ &= \mathbb{E}_{\tilde{Y}_i}[\tilde{Y}_i] \\ &= \mathbb{E} \left[\frac{Y_i + c}{2c} \right] \end{aligned} \quad (5.2)$$

$$= \frac{\mathbb{E}[s + Z_i] + c}{2c} = \left(\frac{s + c}{2c} \right). \quad (5.3)$$

In sharp contrast to the $Q(\cdot)$ function described above, which requires sensors to have the operational ability to resolve any arbitrary bit in the binary expansion of their normalized observations, $Q_{it}^{Th}(\cdot)$

requires only a noisy comparator. Despite the markedly different operational implementations of $Q(\cdot)$ and $Q_{it}^{Th}(\cdot)$ (see (5.1), (2.1), and Fig. 4 which depicts hardware implementations) they are in fact statistically identical: the binary quantized values B_i generated by the two schemes have the same $p_{B_{it}|Y_{it}}(\cdot)$ and $p_{B|s}(\cdot)$ functions where $p_{B_{it}|Y_{it}}(\cdot)$ is the conditional expectation of B_i given $Y_i = y_i$ and $p_{B|s}(\cdot)$ is the unconditional expectation of B_i parameterized by the underlying field value $s(x_i) = s$. These expectations have been evaluated in (5.2), (5.3), (I.1) and (I.2), and we see that for both functions

$$\mathbb{E}[B_i|Y_i = y_i] = p_{B_{it}|Y_{it}}(y_i) = \left(\frac{y_i + c}{2c} \right), \text{ and}$$

$$\mathbb{E}[B_i] = p_{B|s}(s(x_i)) = \left(\frac{s(x_i) + c}{2c} \right).$$

This statistical equivalence allows the two quantization functions $Q(\cdot)$ and $Q_{it}^{Th}(\cdot)$ to be interchanged without affecting the estimation performance.

C. Extensions to Unbounded Noise and Arbitrary Thresholds with Known Distributions

In this work, we have made assumptions of zero-mean, amplitude-bounded, additive noise, which can have an arbitrary, unknown distribution, and uniformly distributed quantization thresholds. The results of this work can be extended to deal with noise that is not amplitude-bounded (i.e. Gaussian, Laplacian, etc.) and for thresholds with arbitrary distributions, however certain technical conditions must be met and the distributions for both the noise and the threshold must be known. A possible approach is to combine the noise and threshold random variables into an overall random dither variable $X_{it} \triangleq Z_{it} + R_{it}$ and applying the method and results used in [2] (see Section V-A). The main MSE result of Theorem 3.1 will still hold, however with new constants multiplying each term in the bound. The method is essentially the same as in Section IV, however the value of the field estimate at every point is passed through a non-linear function, instead of a simple scaling and shifting, given by

$$g(s) = \begin{cases} \mu^{-1}(s) & |s| \leq \mu(a') \\ 0 & \text{otherwise} \end{cases}$$

with $\mu(s) \triangleq 1 - 2P_X(-s)$ where $P_X(\cdot)$ is the cdf of the dither random variable X_{it} . The technical requirement for this extension is that $P_X(\cdot)$ is absolutely continuous with a probability density function $p_X(\cdot)$ on $(-\infty, \infty)$ which is continuous and positive over an open interval $(-a', a')$ containing $[-a, a]$. This ensures that $P_X(\cdot)$ is strictly monotonically increasing over the signal dynamic range and that $\mu^{-1}(\cdot)$ exists (see [2]).

If the sensor observation noise is unbounded (but the field $s_t(x)$ is still bounded), has zero-mean, and has an *unknown* probability density function (pdf) whose tails decay to zero, it is still possible to make a weak statement about the achievable MSE as the number of sensors go to infinity. With unbounded noise, the sensor observations may exceed any finite dynamic range $[-c, c]$ of the one-bit sensors. This leads to the appearance of additional error bias terms (see equation (I.2) and (I.4) in Appendix I) which depend on the unknown signal value $s_t(x)$ to be estimated and the dynamic range limit c . It can be shown that these terms go to zero as $c \rightarrow \infty$. Thus one can assert that for a sufficiently large dynamic range limit c and a corresponding sufficiently large number of sensors $N(c)$, the MSE can be made smaller than some desired tolerance. The actual scaling behavior will now also depend on the tail decay rate of the unknown pdf of the observation noise.

VI. CONCLUDING REMARKS

The results of this work show that for the distributed field reconstruction problem, for every point of continuity of every field snapshot, it is possible to drive the MSE to zero with increasing sensor density while ensuring that the per-sensor bitrate and sensing-related network overhead rate simultaneously go to zero. This can be achieved with noisy threshold (one-bit) comparators with the minimal knowledge of signal and noise dynamic ranges provided that the noise samples are zero-mean, and independent across sensors and the underlying field, and the sensor placement and sampling schedule satisfy a certain uniformity property. The rate of decay of MSE with increasing sensor density is related to the local and global smoothness characteristics of the underlying fields and is order-optimal for the class of spatially constant fields. This work has further clarified the utility of randomization for signal acquisition to combat limited sensing precision and unknown noise statistics in a distributed sensor network context. This work has also attempted to systematically account for sensor placement and hardware issues in addition to the typical constraints encountered in related studies.

ACKNOWLEDGMENT

The authors would like to thank Nan Ma and Manqi Zhao from the ECE department of Boston University for helpful comments and suggestions during different stages of this work. This material is based upon work supported by the US National Science Foundation (NSF) under award (CAREER) CCF-0546598, (CAREER) ECS-0449194, CCF-0430983, and CNS-0435353, and ONR (PECASE) grant no. N00014-02-100362. Any opinions, findings, and conclusions or recommendations expressed in this material are those of the authors and do not necessarily reflect the views of the NSF and ONR.

APPENDIX I
PROOF OF THEOREM 3.1

First, note that the expected value of the binary message B_{it} is given by

$$\begin{aligned}
 \mathbb{E}[B_{it}] &= \mathbb{E}[\mathbf{1}(Y_{it} > R_{it})] \\
 &= \mathbb{E}_{Y_{it}}[\mathbb{E}_{R_{it}}[\mathbf{1}(Y_{it} > R_{it})|Y_{it}]] \\
 &= \mathbb{E}_{Y_{it}}[\mathbb{P}(R_{it} < Y_{it}|Y_{it})] \\
 &\stackrel{(i)}{=} \mathbb{E}_{Y_{it}}\left[\frac{Y_{it} + c}{2c}\right] \tag{I.1}
 \end{aligned}$$

$$\begin{aligned}
 &= \frac{\mathbb{E}[s_t(x_i) + Z_{it}] + c}{2c} \\
 &\stackrel{(ii)}{=} \left(\frac{s_t(x_i) + c}{2c}\right), \tag{I.2}
 \end{aligned}$$

which is the value of the field $s_t(\cdot)$ at location x_i shifted and normalized to the interval $[0, 1]$. Note that the key steps are step (i) where we used the fact that R_{it} is uniformly distributed over $[-c, c]$ and step (ii) where we used the fact that Z_{it} has zero mean. It should be noted that the final result (I.2) holds for any $F_{\mathbf{Z}}(\mathbf{z}) \in \mathcal{F}$.

Using (I.2) we can bound the bias and the variance of the estimator $\hat{S}_t(x)$. The bound on the MSE follows from the bounds on these values since, for any estimator of a non-random parameter, we have

$$\text{MSE}\left(\hat{S}_t(x)\right) = \text{bias}^2\left(\hat{S}_t(x)\right) + \text{var}\left(\hat{S}_t(x)\right). \tag{I.3}$$

Let $j \in \{1, \dots, L\}$ denote the index of the supercell that x falls in. We bound the magnitude of bias

of the estimate $\widehat{S}_t(x)$ in the following way

$$\begin{aligned}
\left| \text{bias} \left(\widehat{S}_t(x) \right) \right| &= \left| \mathbb{E} \left[\widehat{S}_t(x) - s_t(x) \right] \right| \\
&= \left| \mathbb{E} \left[2c \left[\frac{1}{n} \sum_{i \in I(j,t)} B_{it} \right] \right. \right. \\
&\quad \left. \left. - c - s_t(x) \right] \right| \\
&= \left| 2c \left[\frac{1}{n} \sum_{i \in I(j,t)} \mathbb{E} [B_{it}] \right] \right. \\
&\quad \left. - c - s_t(x) \right| \\
&\stackrel{(i)}{=} \left| 2c \left[\frac{1}{n} \sum_{i \in I(j,t)} \left(\frac{s_t(x_i) + c}{2c} \right) \right] \right. \\
&\quad \left. - c - s_t(x) \right| \\
&= \left| \frac{1}{n} \sum_{i \in I(j,t)} (s_t(x_i) - s_t(x)) \right| \\
&\leq \frac{1}{n} \sum_{i \in I(j,t)} |s_t(x_i) - s_t(x)| \\
&\stackrel{(ii)}{\leq} \frac{1}{n} \sum_{i \in I(j,t)} \omega_t (\|x - x_i\|, x) \\
&\stackrel{(iii)}{\leq} \frac{1}{n} \sum_{i \in I(j,t)} \omega_t \left(\frac{\sqrt{d}}{\sqrt[d]{L}}, x \right) \\
&= \omega_t \left(\frac{\sqrt{d}}{\sqrt[d]{L}}, x \right) \\
&\stackrel{(iv)}{\leq} \widetilde{\omega}_t \left(\frac{\sqrt{d}}{\sqrt[d]{L}} \right), \tag{I.4}
\end{aligned}$$

where (i) follows from (I.2), (ii) and (iv) follow from Definitions 2.1 and 2.2, and (iii) follows because the local modulus of continuity is a nondecreasing function of its first argument for each fixed value of its second argument and since any sensor in the supercell containing x is within distance $\frac{\sqrt{d}}{\sqrt[d]{L}}$ of x (the length of the diagonal of a supercell).

The variance of the estimate is bounded by

$$\begin{aligned}\text{var}[\widehat{S}_t(x)] &= \text{var} \left[2c \left[\frac{1}{n} \sum_{i \in I(j,t)} B_{it} \right] - c \right] \\ &= \left(\frac{4c^2}{n^2} \right) \sum_{i \in I(j,t)} \text{var}[B_{it}] \quad (\text{I.5})\end{aligned}$$

$$\leq \left(\frac{4c^2}{n^2} \right) \left(\frac{n}{4} \right) = \left(\frac{LMc^2}{N} \right), \quad (\text{I.6})$$

where we used standard properties of variance and the fact that $\{B_{it}\}$ are independent to obtain (I.5), and we used the fact the variance of a Bernoulli $\{0,1\}$ random variable is bounded by $(1/4)$ and that $n = (N/(LM))$ to obtain (I.6).

Combining these bounds for the bias and variance given in (I.4) and (I.6) of the estimator and using the identity in (I.3), we get the desired bound on the MSE for all $x \in G$, $t \in \{1, \dots, T\}$, and $F_{\mathbf{Z}}(\mathbf{z}) \in \mathcal{F}$.

■

APPENDIX II

PROOF OF THEOREM 3.2

First, we note that

$$\widehat{S}_t(x) \xrightarrow{\text{a.s.}} s_t(x) \equiv \left| \widehat{S}_t(x) - s_t(x) \right| \xrightarrow{\text{a.s.}} 0. \quad (\text{II.1})$$

Thus, we proceed with the triangle equality to bound

$$\begin{aligned} \left| \widehat{S}_t(x) - s_t(x) \right| &\leq \left| \widehat{S}_t(x) - \mathbb{E} \left[\widehat{S}_t(x) \right] \right| \\ &\quad + \left| \mathbb{E} \left[\widehat{S}_t(x) \right] - s_t(x) \right|. \quad (\text{II.2}) \end{aligned}$$

In the proof of Theorem I given in Appendix I we have shown that the second term of (II.2), which is the absolute value of the estimator bias, is bounded by (I.4) which shows that

$$\left| \mathbb{E} \left[\widehat{S}_t(x) \right] - s_t(x) \right| \longrightarrow 0 \quad (\text{II.3})$$

as N and L scale as in (3.1).

Letting j denote the supercell that x falls in, the first term of (II.2) can be rewritten as

$$\left| \widehat{S}_t(x) - \mathbb{E} \left[\widehat{S}_t(x) \right] \right| = \left| 2c \left[\frac{1}{n} \sum_{i \in I(j,t)} B_{it} - \mathbb{E}[B_{it}] \right] \right|.$$

Recall that the cardinality of $I(j, t)$ is $n = (N/(LM))$. Since the B_{it} random variables are independent across sensors and their fourth central moments are uniformly bounded by 1 (since they are binary $\{0, 1\}$ random variables), the strong law of large numbers [27, pp. 206–207] can be applied to obtain

$$\frac{1}{n} \sum_{i \in I(j, t)} B_{it} - \mathbb{E}[B_{it}] \xrightarrow{\text{a.s.}} 0,$$

as $N \rightarrow \infty$ (since $n = (N/(LM))$) and thus the first term of (II.2)

$$\left| \widehat{S}_t(x) - \mathbb{E} \left[\widehat{S}_t(x) \right] \right| \xrightarrow{\text{a.s.}} 0. \quad (\text{II.4})$$

Combining (II.3) and (II.4) into (II.1) and (II.2) finishes the proof. ■

REFERENCES

- [1] E. Masry and S. Cambanis, “Consistent estimation of continuous-time signals from nonlinear transformations of noisy samples,” *IEEE Trans. Info. Theory*, vol. IT-27, pp. 84–96, Jan. 1981.
- [2] E. Masry, “The reconstruction of analog signals from the sign of their noisy samples,” *IEEE Trans. Info. Theory*, vol. IT-27, no. 6, pp. 735–745, Nov. 1981.
- [3] Z. Q. Luo, “Universal decentralized estimation in a bandwidth constrained sensor network,” *IEEE Trans. Info. Theory*, vol. IT-51, pp. 2210–2219, Jun. 2005.
- [4] D. Marco, E. J. Duarte-Melo, M. Liu, and D. Neuhoff, “On the many-to-one transport capacity of a dense wireless sensor network and the compressibility of its data,” in *Information Processing in Sensor Networks, Proceedings of the Second International Workshop, Palo Alto, CA, USA, April 22-23, 2003*, ser. Lecture Notes in Computer Science edited by L. J. Guibas and F. Zhao, Springer, New York, 2003, Apr., pp. 1–16.
- [5] Z. Cvetković and I. Daubechies, “Single bit Oversampled A/D conversion with Exponential accuracy in bit rate,” *Proc. Data Compression Conference*, pp. 343–352, Mar. 2000.
- [6] Z. Cvetković, I. Daubechies, and B. F. Logan, “Interpolation of Bandlimited functions from quantized Irregular Samples,” *Proc. Data Compression Conference*, pp. 412–421, Apr. 2002.
- [7] P. Ishwar, A. Kumar, and K. Ramchandran, “Distributed sampling for dense sensor networks: A “bit-conservation” principle,” in *Information Processing in Sensor Networks, Proceedings of the Second International Workshop, Palo Alto, CA, USA, April 22-23, 2003*, ser. Lecture Notes in Computer Science edited by L. J. Guibas and F. Zhao, Springer, New York, 2003, pp. 17–31.
- [8] A. Kumar, P. Ishwar, and K. Ramchandran, “On distributed sampling of smooth non-bandlimited fields,” in *Proc. Third Intl. Symposium Information Processing in Sensor Networks*. New York, NY: ACM Press, 2004, pp. 89–98.
- [9] T. Berger, Z. Zhang, and H. Viswanathan, “The CEO problem [multiterminal source coding],” *IEEE Trans. Info. Theory*, vol. IT-42, pp. 887–902, May. 1996.
- [10] H. Viswanathan and T. Berger, “The quadratic Gaussian CEO problem,” *IEEE Trans. Info. Theory*, vol. IT-43, pp. 1549–1559, Sep. 1997.
- [11] V. Prabhakaran, D. Tse, and K. Ramchandran, “Rate-region of the quadratic Gaussian CEO problem,” in *Proc. IEEE International Symposium on Information Theory*, Chicago, IL, Jun. 2004, p. 119.

- [12] A. Kashyap, L. A. Lastras-Montano, C. Xia, and Z. Liu, "Distributed source coding in dense sensor networks," in *Proc. Data Compression Conference*, Snowbird, UT, Mar. 2005, pp. 13–22.
- [13] D. L. Neuhoff and S. S. Pradhan, "An upper bound to the rate of ideal distributed lossy source coding of densely sampled data," in *Proc. IEEE International Conference on Acoustics, Speech and Signal Processing*, Toulouse, France, May 2006, pp. 1137–1140.
- [14] Z. Cvetković, "Resilience properties of redundant expansions under additive noise and quantization," *IEEE Trans. Info. Theory*, vol. IT-49, pp. 644–656, Mar. 2003.
- [15] M. Gastpar and M. Vetterli, "Source-channel communication in sensor networks," *Lecture Notes in Computer Science*, vol. 2634, pp. 162–177, Apr. 2003.
- [16] M. Gastpar, B. Rimoldi, and M. Vetterli, "To Code, or not to code: Lossy source-channel communication revisited," *IEEE Trans. Info. Theory*, vol. IT-49, pp. 1147–1158, May 2003.
- [17] R. Nowak, U. Mitra, and R. Willet, "Estimating inhomogenous fields using wireless sensor networks," *IEEE J. Sel. Areas Commun.*, vol. 22, no. 6, pp. 999–1006, Aug. 2004.
- [18] K. Liu, H. El-Gamal, and A. Sayeed, "On optimal parametric field estimation in sensor networks," in *Proc. IEEE/SP 13th Workshop on Statistical Signal Processing*, Jul. 2005, pp. 1170–1175.
- [19] W. Bajwa, A. Sayeed, and R. Nowak, "Matched source-channel communication for field estimation in wireless sensor networks," in *Proc. Fourth Intl. Symposium Information Processing in Sensor Networks*, Apr. 2005, pp. 332–339.
- [20] N. Liu and S. Ulukus, "Optimal distortion-power tradeoffs in Gaussian sensor networks," in *Proc. IEEE International Symposium on Information Theory*, Seattle, WA, USA, Jul. 2006, pp. 1534–1538.
- [21] Q. Zhao, A. Swami, and L. Tong, "The interplay between signal processing and networking in sensor networks," *IEEE Signal Processing Magazine*, vol. 23, no. 4, pp. 84–93, Jul. 2006.
- [22] C. D. Aliprantis and O. Burkinshaw, *Principles of Real Analysis*. San Diego, CA: Academic Press, 1990.
- [23] J. Chou, D. Petrovic, and K. Ramchandran, "Tracking and exploiting correlations in dense sensor networks," in *Proc. Annual Asilomar Conference on Signals, Systems, and Computers*, Pacific Grove, CA, Nov. 2002.
- [24] J. M. Kahn, R. H. Katz, and K. S. J. Pister, "Next century challenges: Mobile networking for "Smart Dust"," in *Proc. ACM International Conference on Mobile Computing and Networking (MOBICOM)*, Seattle, WA, Aug. 1999, pp. 271–278. [Online]. Available: citeseer.nj.nec.com/kahn99next.html
- [25] T. M. Cover and J. A. Thomas, *Elements of Information Theory*, 1st ed. New York, NY: Wiley-Interscience, 1991.
- [26] S. M. Kay, *Fundamentals of Statistical Signal Processing, Volume I: Estimation Theory*, 1st ed. Upper Saddle River, NJ: Prentice-Hall, 1993, vol. 1.
- [27] R. Durrett, *Probability: Theory and Examples*. Thomson Learning College, 1990.